

**Robust Performance Analysis on Active Noise Control
Systems**

T. Bravo and S.J. Elliott

ISVR Technical Memorandum 875

November 2001



SCIENTIFIC PUBLICATIONS BY THE ISVR

Technical Reports are published to promote timely dissemination of research results by ISVR personnel. This medium permits more detailed presentation than is usually acceptable for scientific journals. Responsibility for both the content and any opinions expressed rests entirely with the author(s).

Technical Memoranda are produced to enable the early or preliminary release of information by ISVR personnel where such release is deemed to be appropriate. Information contained in these memoranda may be incomplete, or form part of a continuing programme; this should be borne in mind when using or quoting from these documents.

Contract Reports are produced to record the results of scientific work carried out for sponsors, under contract. The ISVR treats these reports as confidential to sponsors and does not make them available for general circulation. Individual sponsors may, however, authorize subsequent release of the material.

COPYRIGHT NOTICE

(c) ISVR University of Southampton All rights reserved.

ISVR authorises you to view and download the Materials at this Web site ("Site") only for your personal, non-commercial use. This authorization is not a transfer of title in the Materials and copies of the Materials and is subject to the following restrictions: 1) you must retain, on all copies of the Materials downloaded, all copyright and other proprietary notices contained in the Materials; 2) you may not modify the Materials in any way or reproduce or publicly display, perform, or distribute or otherwise use them for any public or commercial purpose; and 3) you must not transfer the Materials to any other person unless you give them notice of, and they agree to accept, the obligations arising under these terms and conditions of use. You agree to abide by all additional restrictions displayed on the Site as it may be updated from time to time. This Site, including all Materials, is protected by worldwide copyright laws and treaty provisions. You agree to comply with all copyright laws worldwide in your use of this Site and to prevent any unauthorised copying of the Materials.

UNIVERSITY OF SOUTHAMPTON
INSTITUTE OF SOUND AND VIBRATION RESEARCH
SIGNAL PROCESSING & CONTROL GROUP

Robust Performance Analysis on Active Noise Control Systems

by

T Bravo and S J Elliott

ISVR Technical Memorandum N° 875

November 2001

Authorised for issue by
Prof S J Elliott
Group Chairman

Acknowledgements

I would like to thank Prof. S. J. Elliott for accepting me as a visiting student in the ISVR for a second time and for his help and advice during the four years of my thesis. To Dr. Cédric Maury and Dr. Paolo Gardonio for the encouragement provided, and to everybody in the ISVR who made my visit there a really pleasant experience. This work has been supported in the form of a studentship from the Ministry of Science and Technology of Spain.

Contents

1. Introduction	1
2. Mathematical formulation of the problem	2
2.1 Perturbed transfer plants	2
2.2 SDP formulation of robust LMS controllers	3
3. Physical application considered	6
3.1 The experimental set-up	6
3.2 Identification of the nominal model	8
4. Simulation results	12
4.1 Estimation of the optimum leak parameter though the resolution of the SDP problem	12
4.2 Estimation of the optimum leak parameter using the measured perturbed plants	14
4.3 Performance results	16
4.4 Another methodology for the solution of the problem	19
5. Robust least squares solution of the problem	22
5.1 Theoretical formulation	22
5.2 Numerical simulations	25
6. Summary and conclusions	27
7. References	28

1. Introduction

It has been shown previously [1] that the multiple-error LMS algorithm is very effective and robust when used for the active control of low-frequency sound and vibration. This algorithm requires an estimation of the response from the secondary sources to the error sensors, which provides a model of the physical system to be controlled. If the estimation does not supply a perfect representation of the true system, the convergence and stability of the algorithm may be affected.

To study these effects on the control system, two different problems concerning the presence of uncertainty in the plant have been considered previously. The first occurs when there are modeling errors in the estimate of the transfer functions, leading to sub-optimal robustness and performance. Second, the model can be accurate but the physical system can vary from the nominal response. It is the second case that has been studied in this work, with the purpose of being aware of how errors can might affect the performance of the active noise control system.

The term uncertainty refers to the differences between the model and the physical system we are dealing with. Both the plant and the primary disturbance can experience uncertainty, which can be classified into structured and unstructured. Boucher et al. [2] have examined the effect of independent random errors in the plant model, that can be due to measurement errors. They introduced a more general cost function that included a term proportional to the mean square effort to stabilise the system. Omoto and Elliott [3] have also investigated the unstructured uncertainties, as well as more structured ones, with dependent changes in the elements of the transfer functions. They obtained a description of the characteristic pattern of the matrices defining the perturbation, which occurred as a result of physical changes in the system under control, due to alteration in the positions of the control sources, error sensors and excitation frequency.

De Fonseca et al. [4] further investigated the effect of both structured and unstructured uncertainties focusing on the design of feedforward control systems exhibiting robust stability and performance. From the mathematical results for robust solutions to least-squares problems with uncertainty data derived by El Ghaoui and Lebret [5], they formulated the stability and performance of the LMS control algorithm as a semidefinite programming (SDP) problem when the data matrices are subject to uncertainty. They presented a SDP formulation for the design of multi-channel LMS algorithms with limited capacity secondary sources, and for the design of

robust LMS algorithms. Although the results they obtained for the synthesis of robust LMS controllers were not new, the SDP formulation of the problem allowed them an optimal choice of the weighting effort control parameter.

In their work, they provide a theoretical method for the design of robust system, however, as they pointed out in the conclusions of the paper, additional work is required to apply the mathematical formulation to real applications. In practice, we need to obtain representations of the uncertainty which provides a proper description of the system in a way that facilitates convenient manipulation.

Some previous work has been done previously in the ISVR [6] to control low frequency harmonic noise in a rectangular enclosure when the physical plant varied from the nominal state. In that work these effects were studied in relation with the placement of transducers in the active noise control system. It is the purpose of this research to extend the previous analysis of De Fonseca et al. [4] and apply some of his mathematical conclusions. Previous results can be used as a starting point and compared with the ones obtained using the theoretical formulation.

The rest of the report is structured as follows: Section 2 summarises the relevant theoretical results for the SDP formulation of the problem which will be used in the real system; Section 3 reviews the experimental set-up used previously to investigate the control of low tonal frequency noise in an enclosure and the results obtained; Section 4 shows the simulation results obtained with this particular application and Section 5 expounds a robust least squares solution for the problem. Finally, some conclusions are discussed in the last section.

2. Mathematical formulation of the problem

2.1 Perturbed transfer plants

We cannot predict exactly what the output of a real physical system will be even if we know the input, so we are uncertain about the system. Whatever formulation is used to express these errors is a representation of uncertainty.

Control designs are based on the use of a model, whether from theoretical predictions or experimental measurements. Since a fixed model can not respond to the variations that can occur in the true plant, we need at least a set of maps that allow for plant dynamics that are not explicitly represented in the model structure.

The basic technique is to model the plant as belonging to a set that can be either structured or unstructured. For example, we can consider our problem assuming that the uncertainty is generated by an additive noise signal with a bounded norm. Of course, no physical system is linear with additive noise, but some aspects of the physical behaviour are approximated satisfactorily using this model.

For each element of the perturbed transfer function matrices a part will be constant and a part will be unknown, so the measured plant, \mathbf{G} can be represented as having a nominal part \mathbf{G}_0 and an additive uncertainty $\Delta\mathbf{G}$, so that

$$\mathbf{G} = \mathbf{G}_0 + \Delta\mathbf{G} \quad (1)$$

In the unstructured perturbation case, we can express the additive perturbation function in terms of a fixed weighting factor, ρ , and a variable matrix Δ satisfying $\|\Delta\| \leq 1$. In this work, the maximum singular value norm is used for matrix norms, and the Euclidean norm for vectors. Equation (1) can then be expressed as

$$\begin{aligned} \mathbf{G} &= \mathbf{G}_0 + \rho\Delta \\ \|\Delta\| &\leq 1 \end{aligned} \quad (2)$$

This inequality describes a disk in the complex plane: at each frequency, the measure plant, \mathbf{G} , lies in the sphere with radius ρ and centre \mathbf{G}_0 . There is a bound on the independent perturbation block, Δ , determined by his maximum singular value norm. The parameter ρ is the perturbation size. In order to use this uncertainty model it is necessary to characterised a nominal plant of the system, \mathbf{G}_0 , and the weighting parameter ρ .

2.2 SDP formulation of robust LMS controllers

De Fonseca et al. [4] analyse the robust performance and robust stability problems as convex semidefinite programming (SDP) problems, formulated as the minimisation of a real linear objective function of a vector of variables $\mathbf{x} \in \mathbb{R}^m$, subject to linear real-valued matrix inequality (LMI) constraints

$$\begin{aligned} \min \mathbf{c}^T \mathbf{x} \\ s.t. \mathbf{F}(\mathbf{x}) \geq 0, \end{aligned} \quad (1)$$

where

$$\mathbf{F}(\mathbf{x}) \equiv \mathbf{F}_0 + \sum_{i=1}^m \mathbf{x}_i \mathbf{F}_i \quad (2)$$

The problem is defined by the vector $\mathbf{c} \in \mathcal{R}^m$ and the $m+1$ symmetric matrices $\mathbf{F}_0, \dots, \mathbf{F}_m \in \mathcal{R}^{n \times n}$. The inequality sign in equation (1) means that $\mathbf{F}(\mathbf{x})$ is positive semidefinite.

Let's consider now the formulation of the robust performance of the LMS controller in an active noise control system as an SDP problem. Assuming that L sensors positions and M secondary sources have been determined previously, the sound field at the microphones positions can be written as the contribution due to the primary source plus the contributions due to the secondary sources

$$\mathbf{e} = \mathbf{d} + \mathbf{G} \mathbf{u} \quad (3)$$

where \mathbf{e} is a $L \times 1$ complex vector of error signals, \mathbf{d} is a $L \times 1$ complex vector of error signals due to the primary sources, \mathbf{G} is a $L \times M$ complex transfer matrix from the secondary sources to the error sensors and \mathbf{u} is a $M \times 1$ complex vector of secondary source strengths. A suitable cost function can be defined as the sum of the modules squared error pressures

$$\sigma = \mathbf{e}^H \mathbf{e} \quad (4)$$

which can also be written as

$$\sigma = \|\mathbf{d} + \mathbf{G} \mathbf{u}\| \quad (5)$$

The corresponding minimum value of this quadratic cost function is given by [7]

$$\sigma_o = \mathbf{d}^H [\mathbf{I} - \mathbf{G}(\mathbf{G}^H \mathbf{G})^{-1} \mathbf{G}^H] \mathbf{d} \quad (6)$$

The attenuation value for a fixed configuration used through this report is defined as

$$Attenuation(dB) = 10 \log_{10} \left(\frac{\mathbf{d}^H \mathbf{d}}{\sigma_o} \right) = 10 \log_{10} \left(\frac{\mathbf{d}^H \mathbf{d}}{\mathbf{d}^H [\mathbf{I} - \mathbf{G}(\mathbf{G}^H \mathbf{G})^{-1} \mathbf{G}^H] \mathbf{d}} \right) \quad (7)$$

which gives a measure of the noise reduction in the microphones positions after the introduction of the active noise control system.

Considering the in-phase and quadrature components of the complex error, $\mathbf{e} = \mathbf{e}_R + j\mathbf{e}_I$, equation (3) can be written in the entirely real form

$$\mathbf{e} = \begin{bmatrix} \mathbf{e}_R \\ \mathbf{e}_I \end{bmatrix} = \begin{bmatrix} \mathbf{d}_R \\ \mathbf{d}_I \end{bmatrix} + \begin{bmatrix} \mathbf{G}_R & -\mathbf{G}_I \\ \mathbf{G}_I & \mathbf{G}_R \end{bmatrix} \begin{bmatrix} \mathbf{u}_R \\ \mathbf{u}_I \end{bmatrix} \quad (8)$$

so

$$\sigma = \mathbf{e}^T \mathbf{e} \quad (9)$$

Assume now that the secondary path transfer function matrix, \mathbf{G} , and the primary vector, \mathbf{d} , are subject to perturbations. The perturbed system can be expressed as

$$[\mathbf{G}\mathbf{d}] = [\mathbf{G}_0 \mathbf{d}_0] + \rho \Delta \quad \text{with } \Delta = [\Delta \mathbf{G} \Delta \mathbf{d}] \quad \text{and } \|\Delta\| \leq 1 \quad (10)$$

El Ghaoui and Lebret [5] have defined the worst-case residual for a fixed control signal vector as

$$\sigma(\mathbf{G}_0, \mathbf{d}_0, \rho, \mathbf{u}) = \max_{\|\Delta\| \leq \rho} \|(\mathbf{G}_0 + \Delta \mathbf{G})\mathbf{u} + (\mathbf{d}_0 + \Delta \mathbf{d})\| \quad (11)$$

They consider that the control signal is a robust least square solution if it minimises the worst-case residual $\sigma(\mathbf{G}_0, \mathbf{d}_0, \rho, \mathbf{u})$, as

$$\sigma_{opt}(\mathbf{G}_0, \mathbf{d}_0, \rho) = \min_{\mathbf{u}} \max_{\|\Delta\| \leq \rho} \|(\mathbf{G}_0 + \Delta \mathbf{G})\mathbf{u} + (\mathbf{d}_0 + \Delta \mathbf{d})\| \quad (12)$$

This solution trades accuracy for robustness at the expense of introducing bias. Using Schur complements, this problem is converted into an SDP formulation as

$$\begin{aligned}
& \min_{\sigma, \tau, \mathbf{u}} \sigma \\
& \text{s.t.} \quad \begin{bmatrix} (\sigma - \tau)\mathbf{I} & (\mathbf{G}_0 \mathbf{u} + \mathbf{d}_0) \\ (\mathbf{G}_0 \mathbf{u} + \mathbf{d}_0)^T & (\sigma - \tau) \end{bmatrix} \geq 0 \\
& \quad \quad \begin{bmatrix} \mathbf{d} & \rho \begin{bmatrix} \mathbf{u} \\ 1 \end{bmatrix} \\ \rho [\mathbf{u} \quad 1] & \tau \end{bmatrix} \geq 0
\end{aligned} \tag{13}$$

At the optimum, the variable τ takes the following value

$$\tau_{opt} = \rho \sqrt{\|\mathbf{u}\|^2 + 1} \tag{14}$$

The solution to this problem is given by

$$\mathbf{u} = \begin{cases} -(\mu \mathbf{I} + \mathbf{G}_0^T \mathbf{G}_0)^{-1} \mathbf{G}_0^T \mathbf{d}_0 & \text{if } \mu \equiv \rho^2 \frac{(\sigma - \tau)}{\tau} > 0, \\ -\mathbf{G}_0^+ \mathbf{d}_0 & \text{else } (\mu = 0) \end{cases} \tag{15}$$

The parameter μ is the solution of the DSP problem, with respect to the perturbation size of the particular problem. The formulation of the problem in this way allows an optimal choice, from a robustness point of view, for this leak parameter, which can also be shown to be the parameter controlling the effort weighting in a modified cost function [11]. This is the theoretical result that will be applied to a real case in the next section.

3. Physical application considered

3.1 The experimental set-up

The first step to study the robust performance problem is the determination of an appropriate data set of the uncertainty that can appear in the physical problem to be considered. The system under study in this work consisted of a wooden laboratory mock-up of an aircraft interior with internal dimensions $L_x=2.1\text{m}$, $L_y=6.0\text{m}$ and $L_z=2.1\text{m}$. This enclosure was initially constructed to analyse the main features of the field inside an aircraft. The enclosure characteristics have been widely described [7] and will no be examined here again.

A multichannel active control system was installed in the enclosure with 32 error signals from electret microphones and 16 secondary control outputs to 200-mm loudspeakers. The error

sensors were uniformly distributed in an 8x4 grid inside the enclosure at head height. The primary acoustic field is a pure tone at 88 Hz, generated by a 300 mm diameter loudspeaker driven from an oscillator which also provides the reference signal for the control system. The approximated positions of the transducers in the enclosure are indicated in Figure 1.

The electronic controller implements the Multiple Channel LMS Algorithm. This algorithm minimises a cost function taking into account the sum of the mean-square signals from the error sensors and the sum of the mean-square signals fed to the secondary sources. In order to perform the simulations, it is necessary to use the control system to measure the transfer functions from each secondary source to each error sensor and to measure the primary field at the error sensor positions. These data have been used in the simulations performed through this work.

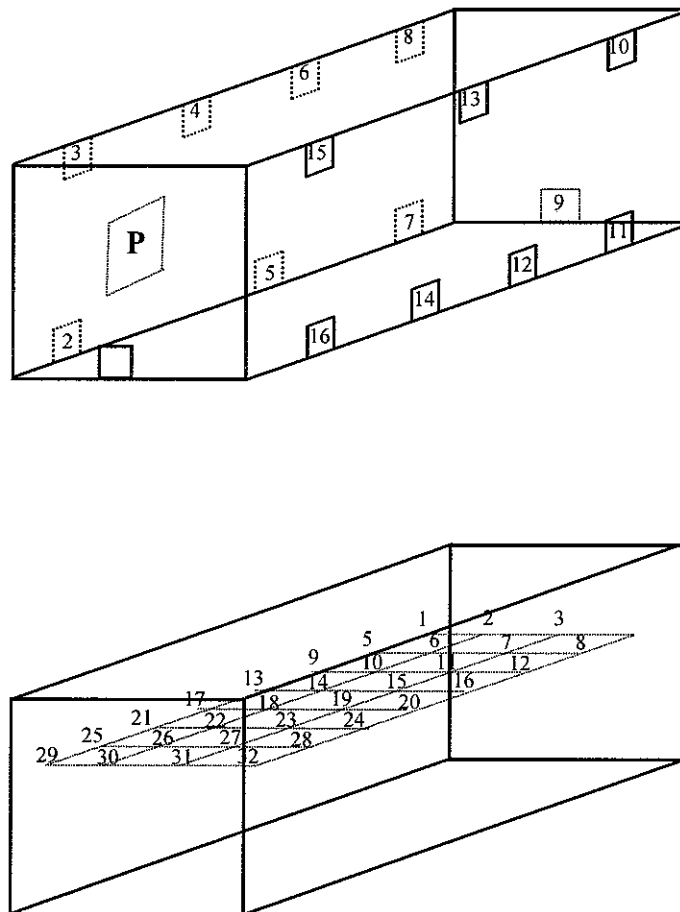


Figure 1. Loudspeaker and microphone positions in the laboratory enclosure

To investigate the robustness of the control system when changes occur in the plant, six different perturbed plants, corresponding to six different situations that could happen in practice, were measured in the laboratory enclosure. These matrices were:

\mathbf{G}_1 : Occupants standing under the error microphones.

\mathbf{G}_2 : The same that \mathbf{C}_1 but two persons walking along a central corridor

\mathbf{G}_3 : Occupants walking over the whole enclosure

\mathbf{G}_4 : Occupants walking along a central corridor

\mathbf{G}_5 : Occupants sitting down under the error microphones

\mathbf{G}_6 : The same that \mathbf{C}_5 but two persons walking along a central corridor

In a previous work [6] the research was focused in the selection of the transducer positions that minimised the average of this set of cost functions to obtain locations whose performance were robust to operating changing conditions. The same set of data will be used in this work to represent the models that allow for plant dynamics which are not explicitly represented in the nominal structure, necessary to apply the theoretical results in a practical situation. It is expected that the performance objectives would be satisfied for every plant represented by this perturbed data set.

3.2 Identification of the nominal model

The theoretical framework for the formulation of the robust performance analysis assumes that the data matrices \mathbf{G}_0 and \mathbf{d}_0 are the nominal values of the model, which are subject to perturbations bounded in norm by ρ . Now, if we think of these data as measured data, the assumption that the measured plants \mathbf{G}_i correspond to the nominal model may not be judicious, and it would be necessary to build a nominal representation of the observed set.

A computational algorithm was used to find the size of the perturbation ρ that minimises the difference in the norms between the nominal plant and the perturbed ones. To obtain a first approximation we choose each one of the perturbed plants, \mathbf{G}_i , as the nominal plant, \mathbf{G}_{0i} , and calculate the differences in the norm between all the others, as

$$\|\Delta \mathbf{G}_j\| = \|\mathbf{G}_j - \mathbf{G}_{0i}\|, \quad i, j = 1, 2, \dots, 6 \quad (16)$$

The results obtained with the six experimental perturbed plant in the laboratory enclosure, using 16 secondary sources and 32 microphones, are summarised in Table 1.

Table 1. Differences in the norm between the perturbed measured transfer functions in a laboratory enclosure and maximum values obtained for each set

	$\ \Delta \mathbf{G}_1\ $	$\ \Delta \mathbf{G}_2\ $	$\ \Delta \mathbf{G}_3\ $	$\ \Delta \mathbf{G}_4\ $	$\ \Delta \mathbf{G}_5\ $	$\ \Delta \mathbf{G}_6\ $
\mathbf{G}_1	0	0.0818	0.0880	0.0828	0.1849	0.1478
\mathbf{G}_2	0.0818	0	0.0890	0.0908	0.1816	0.1421
\mathbf{G}_3	0.0880	0.0890	0	0.0769	0.1823	0.1504
\mathbf{G}_4	0.0828	0.0908	0.0769	0	0.1859	0.1544
\mathbf{G}_5	0.1849	0.1816	0.1823	0.1859	0	0.0802
\mathbf{G}_6	0.1478	0.1421	0.1504	0.1544	0.0802	0
max	0.1849 ₍₁₋₅₎	0.1816 ₍₂₋₅₎	0.1823 ₍₃₋₅₎	0.1859 ₍₄₋₅₎	0.1859 ₍₅₋₄₎	0.1544 ₍₆₋₄₎

Once all the norms of the differences have been calculated, the first approximation for the value of ρ and the corresponding value of \mathbf{G}_0 are selected taking into account the maximum difference encountered so far, that corresponds, as can be seen in Table 1, to the difference in the norm between the forth and the fifth measured transfer functions. Selecting the medium point of these two matrices as the nominal matrix, the first iteration values are given by

$$\rho_{(1)} = \frac{\|\Delta \mathbf{G}_{4-5}\|}{2} \quad (17)$$

$$\mathbf{G}_{0(1)} = \frac{\mathbf{G}_4 + \mathbf{G}_5}{2}$$

The next step in the algorithm corresponds to checking if the rest of the perturbed plants are included in the *circle* with ratio $\rho_{(1)}$ and centre $\mathbf{G}_{0(1)}$. If so, the values for the size of the perturbation and the nominal function transfer matrix expressed in equation (4) are the exact solutions of the problem. Again, the differences in the norm are calculated using the nominal plant $\mathbf{G}_{0(1)}$ and the six perturbed plants \mathbf{G}_i . These result and the values for the perturbation block, Δ_i , for the corresponding $\rho_{(1)}$ radius are summarised in the first two columns in Table 2. From the analysis of the values obtained for the perturbed block, Δ_i , using the first approximation of the nominal plant, $\mathbf{G}_{0(1)}$, and the parameter $\rho_{(1)}$, it can be seen that there are matrices just outside this *circle*, as these values are not bounded by unity norm. To include all the perturbed plants inside, it is necessary to select a new approximation to ρ as the maximum

value for all the $\Delta \mathbf{G}_i$ encountered. This value has been outlined in the last row, and has been chosen as the second iteration for the radius of the *circle*. The new perturbed block values obtained with $\rho_{(2)}$ are shown in the third column in Table 2.

Table 2. Differences in the norm between the perturbed measured transfer functions and the nominal plant $\mathbf{G}_{0(1)}$, and the values obtained for the perturbed block for different selections of ρ

	$\ \Delta \mathbf{G}_i\ $	$\Delta_i(\rho_{(1)} = 0.0930)$	$\Delta_i(\rho_{(2)} = 0.0953)$
\mathbf{G}_1	0.0949	1.0213	0.9958
\mathbf{G}_2	0.0937	1.0076	0.9824
\mathbf{G}_3	0.0953	1.0256	1.0000
\mathbf{G}_4	0.0930	1.0000	0.9750
\mathbf{G}_5	0.0930	1.0000	0.9750
\mathbf{G}_6	0.0868	0.9344	0.9110
max	0.0953 ₍₃₎	1.0256 ₍₃₎	1.0000 ₍₃₎

In this way, we have established one upper and lower limit for the optimal value of the perturbation size as

$$\rho_{(1)} = 0.0930 < \rho \leq \rho_{(2)} = 0.0953 \quad (18)$$

The following steps in the algorithm to find the optimum perturbation size are:

1. Choose a *point* situated between the perturbed plants as the nominal plant, \mathbf{G}_0 , (for example the average), calculate the difference in the norms between the nominal plant and the perturbed plants and select the largest one.
2. Move the nominal plant \mathbf{G}_0 towards the *furthest* perturbed matrix, $\mathbf{G}_{\text{furthest}}$, calculating the difference in the norms for each iteration, until you find another *point* at the same distance (in the maximum singular value norm sense) from the nominal plant.
3. Check if there are still more point situated at the same distance from the nominal plant \mathbf{G}_0 . If so, we have found the exact solution, because the optimal circle has to pass at least though three points. If not, find again the next largest distance from \mathbf{G}_0 . The point situated at the same distance from these three selected perturbed matrices gives the optimal solution to the problem.

The final solution provided by the algorithm for the differences in the norm, and the perturbed blocks for the six measured transfer functions are summarised in Table 3. The perturbation size is determined as being $\rho = 0.0941$.

Table 3. Differences in the norm between the perturbed measured transfer functions and the nominal plant in a laboratory enclosure, and the values obtained for the perturbed block for the final values provided by the algorithm

	$\ \Delta G_i\ $	$\Delta_i (\rho=0.0941)$
G_1	0.0941	1.0000
G_2	0.0925	0.9837
G_3	0.0941	1.0000
G_4	0.0919	0.9765
G_5	0.0941	1.0000
G_6	0.0872	0.9274
max	0.0941	1.0000

Using this algorithm, the size of the additive uncertainty, ρ , has been calculated as a function of the number of secondary sources used in the control system. The particular configurations used for the simulation results have been selected by the simulated annealing method [8] in a previous work [6] as those that provide the greatest attenuation for the average combination of the six perturbed transfer functions. The results obtained are shown in Figure 2.

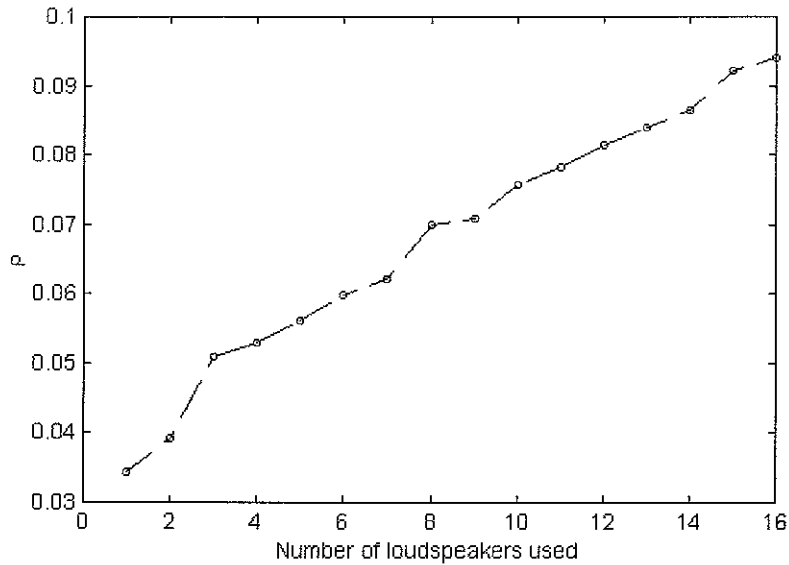


Figure 2. Size of the perturbation uncertainty as a function of the number of secondary sources used in the experimental enclosure

As it can be expected, the size of the perturbation uncertainty increases as the number of secondary sources included in the active noise control system in the enclosure grows. It should be noted that the norm of G_0 also increases as the number of loudspeakers gets larger, and so the normalised perturbation remains about the same. Once we have obtained the nominal plant and the perturbation size for the best combinations of secondary sources in the

experimental set-up, we can analyse the robust performance for the active control system. These results are presented in the following sections.

4. Simulation results

4.1 Estimation of the optimum leak parameter through the resolution of the SDP problem

The resolution of the SDP problem formulated in Section 2.2 can be carried out in an efficient way using the developed interior point methods [9]. In the simulations presented in this work, the software package SDPT3 has been used. This software is an implementation of infeasible path-following algorithms and homogeneous and self-dual methods for solving standard semidefinite programs (SDP) developed by Toh et al. [9]. The implementation exploits the block-diagonal structure of the given data, and offers four types of search direction, which is best suited the particular application considered. The algorithm is very efficient and robust, but its performance is quite sensitive to the choice of the initial iterate, and it is desirable to choose an initial iterate that has at least the same order of magnitude as an optimal solution of the SDP.

To select the optimal values for the effort control coefficient, in equation (12), we need to express the problem in the form of equations (1) and (2). The vector of unknowns \mathbf{x} , will contains σ, τ , and the components of \mathbf{u} . The vector \mathbf{c} only contains one 1 to select σ from the vector of unknowns \mathbf{x} , so that

$$\begin{aligned}\mathbf{x} &= (\sigma, \tau, u_1, u_2, \dots, u_{16})^T \\ \mathbf{c} &= (1, 0, \dots, 0)\end{aligned}$$

Combining the constraint matrices in blocks into the \mathbf{F}_i matrices, the problem can be expressed as

$$\begin{aligned}\min \mathbf{c}^T \mathbf{x} \\ \text{s.t. } \mathbf{F}_0 + \sigma \mathbf{F}_\sigma + \tau \mathbf{F}_\tau + u_1 \mathbf{F}_{u_1} + u_2 \mathbf{F}_{u_2} + \dots + u_{16} \mathbf{F}_{u_{16}} \geq 0,\end{aligned}\tag{19}$$

Solving now the SDP problem for a range of values of ρ , we can obtain the optimum leak parameter μ , from a robustness point of view, as a function of the perturbation size. The results for the enclosure in Figure 1, with 16 secondary loudspeakers and 32 error microphones, are shown in Figure 3. For the measured perturbation size of 0.094 this graph predicts that a leak parameter of about 10^{-3} must be used to ensure that the adaptive algorithm is robustly stable.

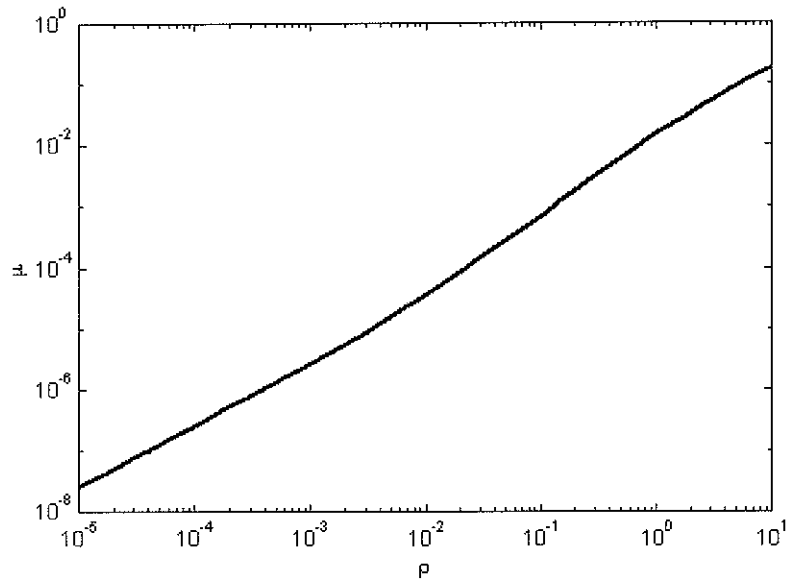


Figure 3. Optimal effort coefficient μ vs. perturbation size ρ

As it could be expected, the optimal leak parameter, μ , increases as the size of the perturbation is higher. To validate the results obtained in terms of performance, it would be necessary to calculate the optimum effort coefficient for different numbers of loudspeakers selected by means of the simulated annealing algorithm. Using the values of the perturbation size represented in Figure 2, the SDP algorithm has been used again to find the optimal values of μ . The results are presented in Figure 4, for the different numbers of secondary sources used in the control system.

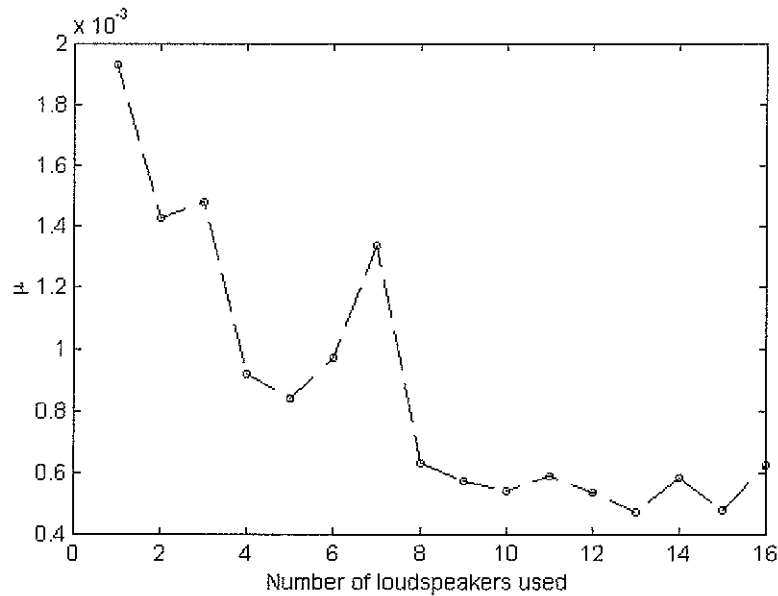


Figure 4. Optimal values of the effort weighting coefficient μ vs. number of secondary sources used

As it can be seen, the values of the optimal effort weighting coefficient are much higher when a small number of loudspeakers is used in the control system, and remain almost constant from 10 loudspeakers to the total number. This variation shows the opposite trend to the attenuation values obtained in the previous work [6], that increase with a high rate at the beginning, until for about 10 loudspeakers they provide an attenuation which is almost as good as the value obtained with the 16 loudspeakers.

4.2 Estimation of the optimum leak parameter using the measured perturbed plants

In order to be confident in the results obtained with the software package, and especially, in the tuning of the characteristic parameters and the selection of the different direction methods provided, an estimation of the optimal value of the leak coefficient was carried out directly with the six measured transfer plants in the enclosure.

For each of the measured perturbed plants we can express the vector of error signals as

$$\mathbf{e}_i = \mathbf{d}_i + \mathbf{G}_i \mathbf{u} \quad (20)$$

From the mathematical solution of the SDP problem, equation (12), we have found that the optimum control input vector signal that minimises the squared error signal in the face of uncertainty in the system is given by

$$\mathbf{u} = -(\mu \mathbf{I} + \mathbf{G}_0^H \mathbf{G}_0)^{-1} \mathbf{G}_0^H \mathbf{d}_0 \quad (21)$$

Substituting this expression into the signal error vector, we have

$$\mathbf{e}_i = \mathbf{d}_i - \mathbf{G}_i (\mu \mathbf{I} + \mathbf{G}_0^H \mathbf{G}_0)^{-1} \mathbf{G}_0^H \mathbf{d}_0 \quad (22)$$

Defining now a cost function as the sum of the square error vector signals, $\sum_{i=1}^6 \mathbf{e}_i^H \mathbf{e}_i$, we can then make an estimation of the optimum leak parameter, μ , considering the six measured perturbed plants. The variation of this cost function as a function of the leak parameter is

represented in Figure 5, when 16 secondary sources and 32 error sensors are used in the control system.

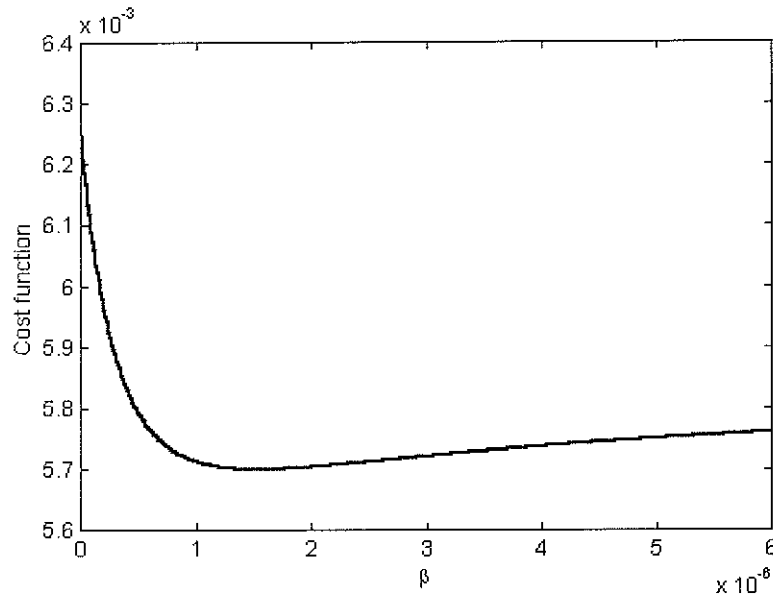


Figure 5. The sum of the square error signals for the six perturbed plants in the enclosure as a function of the leak parameter, μ

From this figure we can select the value of μ that provides the minimum residual error signal. If we repeat the same procedure for the best combinations selected by the simulated annealing algorithm, for the different number of secondary sources that can be used in the experimental enclosure, we can obtain a representation of the optimum effort control coefficient as a function of the loudspeakers in the control system. This is represented in Figure 6.

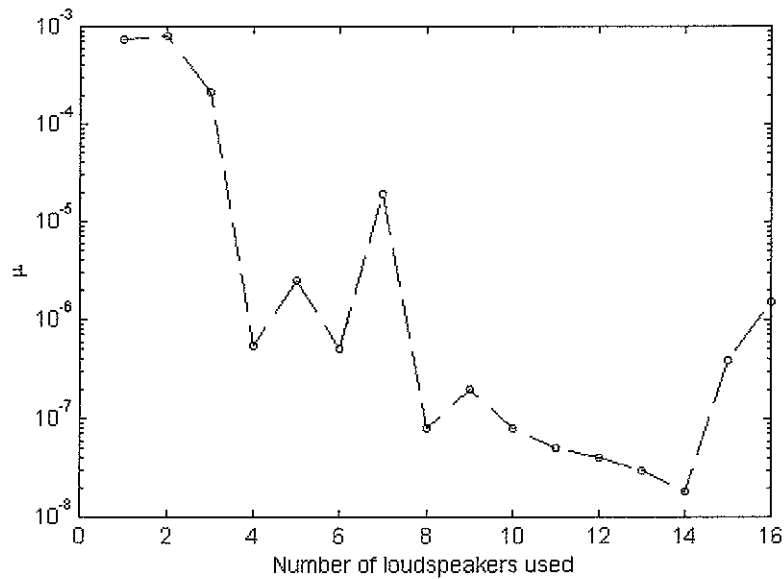


Figure 6. Optimal estimated values of the effort coefficient μ vs. number of secondary sources used in the active control system

Before making a comparison between Figure 4, when the values of μ are calculated solving the SDP problem, and Figure 6, when the values of the leak parameter are estimated from the six perturbed transfer plants, it is necessary to point out that a semilogarithm representation has been used for μ in this case. The shape of the figures is very similar, both of them show the same trend, but the difference between them are much more dramatic in the second case, and the values of the leak parameter are smaller when estimated from the six perturbed plant, than from the solution of the SDP problem. This is expected because the first case only used the nominal plant and the size of the perturbation for the solution of the problem which is assumed to be completely unstructured, and the optimal effort coefficient obtained is absolutely general, whereas in the second case we are estimating a value of μ using a reduced set composed of six measurements, whose variation will have the same structure.

4.3 Performance results

To validate the results obtained with the SDP formulation in terms of robustness for the problem, numerical simulations have been performed to calculate the attenuation values provided in different situations. In all the simulations, the optimum control input vector signal that minimises the squared error signal is the one expressed in equation (18), from the theoretical solution of the robustness problem. Several definitions of residual error signals have been used in this study. Using first the nominal plant, obtained using the computational algorithm described in Section 3.2, the vector of error signals is equal to

$$\mathbf{e}_0 = \mathbf{d}_0 + \mathbf{G}_0 \mathbf{u} \quad (23)$$

and substituting equation (18) into equation (20), we obtain the residual vector of error signal

$$\mathbf{e}_0 = \mathbf{d}_0 - \mathbf{G}_0 \left(\mu \mathbf{I} + \mathbf{G}_0^T \mathbf{G}_0 \right)^{-1} \mathbf{G}_0^T \mathbf{d}_0 \quad (24)$$

The fitness function used as a measure of the performance, is defined as in equation (6)

$$Attenuation = 10 \log_{10} \left(\frac{\mathbf{d}_0^H \mathbf{d}_0}{\mathbf{e}_0^H \mathbf{e}_0} \right) \quad (25)$$

The values obtained using the nominal primary field and the nominal error signal are represented in Figure 7 for two different situations. The results obtained for the “nominal” situation, when the leak parameter, μ , is set to zero are shown in the circle-dot line, while those obtained when the effort weighting coefficient μ takes the optimum values obtained mathematically, as shown in Figure 4, are represented by the point-dashed line.

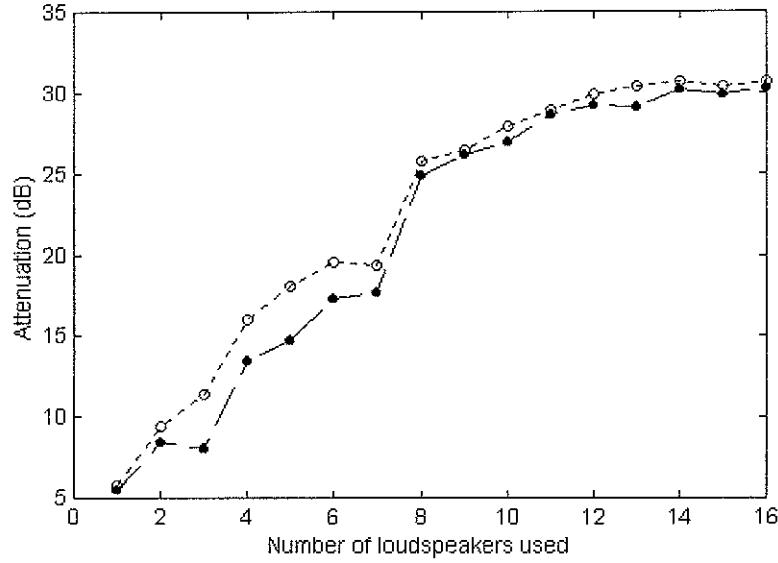


Figure 7. Attenuation values obtained as a function of the number of loudspeakers used in the active control system for the nominal plant. Effort parameter value μ equal to zero: circle-dot line; optimal values of μ in terms of performance: point-dashed line

As it could be predicted, the attenuation values obtained for the “nominal” plant, when the leak parameter has not been included, provide slightly better results than those when the effort coefficient differs from zero, but with at least eight loudspeakers the reduction in performance is less than about 1 dB when the leak is included. It is necessary to check now what happens when perturbation is introduced in the system. The equations corresponding to the measured perturbed plants have been already deduced in Section 4.2. Using again the same value of the optimum complex vector of secondary source strengths, equation (21), the residual signal of error sensor are given by equation (22)

$$\mathbf{e}_i = \mathbf{d}_i - \mathbf{G}_i \left(\mu \mathbf{I} + \mathbf{G}_0^T \mathbf{G}_0 \right)^{-1} \mathbf{G}_0^T \mathbf{d}_0 \quad (22)$$

where each \mathbf{d}_i and \mathbf{G}_i are taken from the set listed in Section 3.1. The attenuation values in this case are defined to be

$$Attenuation = 10 \log_{10} \left(\frac{\sum_{i=1}^6 \mathbf{d}_i^H \mathbf{d}_i}{\sum_{i=1}^6 \mathbf{e}_i^H \mathbf{e}_i} \right) \quad (26)$$

The results obtained using the perturbed plants are represented in Figure 8 in analogous manner to Figure 7, so the comparison can be easily made.

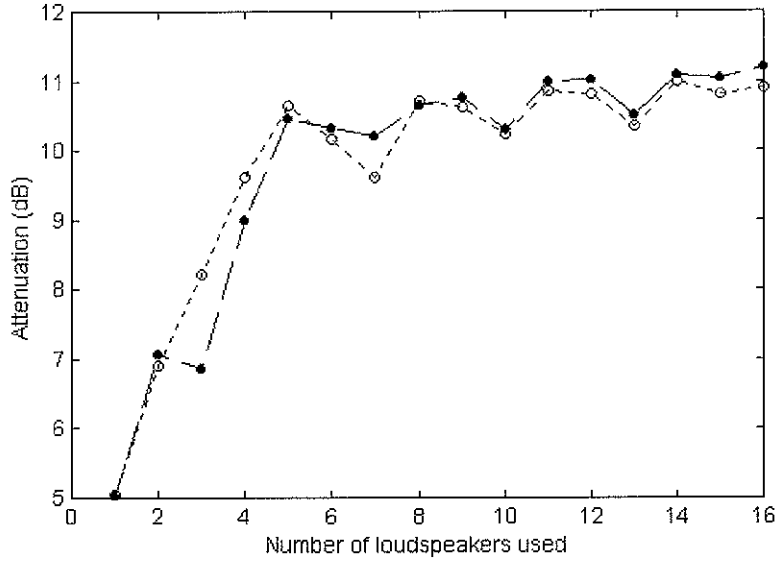


Figure 8. Attenuation values obtained as a function of the number of loudspeakers used in the active control system using the perturbed plants. Effort parameter value μ equal to zero: circle-dot line; optimal values of μ in terms of performance: point-dashed line

As it can be seen, in general the results are now better using the “robust” solution, when the leak parameter has been obtained with the SDP formulation of the problem, than those achieved with the “nominal” solution, when μ is set to zero. It is interesting to note the important difference between the attenuation values in Figures 7 and 8. When uncertainty appears in the system, the attenuation decreases so that it is less than half of the value obtained using the nominal plant. In the previous work [6], when only the perturbed plants were considered in the average cost function, it was found that the results were only very slightly smaller than when using the nominal plant. In this case, it is supposed that all the perturbed plants represented by the nominal plant and the perturbation size are included in the robustness problem, and the cancellation values are much smaller.

4.4 Another methodology for the solution of the problem

The criterion used in the previous sections to determine the loudspeaker positions is based on using an average of the perturbed plants as a cost function in the simulated annealing algorithm [9]. For each one of these combinations with different number of secondary sources, the computational algorithm in Section 3.2 has been used to obtain the corresponding nominal plant and perturbation size for these particular configurations.

In this section, the starting point is again the measured perturbed plants, but these are used to determine the nominal plant only for the total number of loudspeakers that can be used in the control system. Once the nominal data has been obtained, the simulated annealing is applied to select the best positions when the number of secondary sources varies from one to the total number. The cost function used by the simulated annealing algorithm in this case is the attenuation obtained by the control system, taking into account the nominal plant, as defined in equation (6). The maximum attenuation values achieved, the control effort and the selected combination for each set of loudspeakers, from 1 to 16 are shown in Table 1. The attenuation values are represented in Figure 9 in point-dashed line. For comparison, in the same figure are also represented the values obtained previously for the nominal plant, but for the positions optimise for the perturbed plants, in circle-dotted line.

Table 1. Best attenuation values for the problem of finding M loudspeakers positions, where M varies from 1 to 16, with the corresponding control effort values and the selected configurations, for the nominal plant

Total No. of loudspeakers	Attenuation (dB)	Total control effort	Loudspeaker positions
1	5.5799	0.9575	0000000000000010
2	8.8310	0.8986	0010000000000010
3	12.5693	3.8888	0110000000000001
4	16.0161	3.9452	1010100000000001
5	19.0668	2.0668	0101100000010100
6	21.8828	2.0351	0101101000010100
7	25.3757	1.9297	0101101010010100
8	27.0299	1.8728	0101111010010100
9	28.2305	1.7266	0101111010010101
10	28.7913	2.9830	1001111010011101
11	29.8351	2.6887	1001111010011111
12	30.1643	2.5688	1001111100111111
13	30.6089	2.7608	1011111110011111
14	30.6473	2.1953	1111111110011111
15	30.7050	2.2696	1111111110111111
16	30.7158	2.3881	1111111111111111

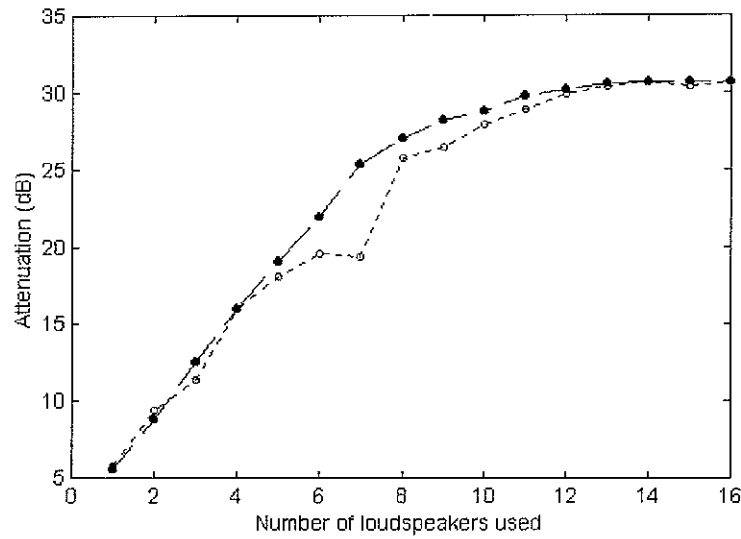


Figure 9. Attenuation values obtained as a function of the number of loudspeakers used in the active control system for the nominal plant. Optimal positions based on the perturbed plants: circle-dot line; optimal positions based on the nominal plant: point-dashed line

This figure is a confirmation that the attenuation values for the nominal plant are better when the same plant is used by the optimisation algorithm, than when the set of perturbed plant has been used for the selection of the best transducer positions. Once the algorithm has selected the best combinations, the same set of loudspeakers is selected for the perturbed plants, and the perturbation size is calculated as the largest difference in norm between the nominal and the corresponding perturbed plants. The values obtained are represented in Figure 10, as well as the previous values obtained in Figure 2.

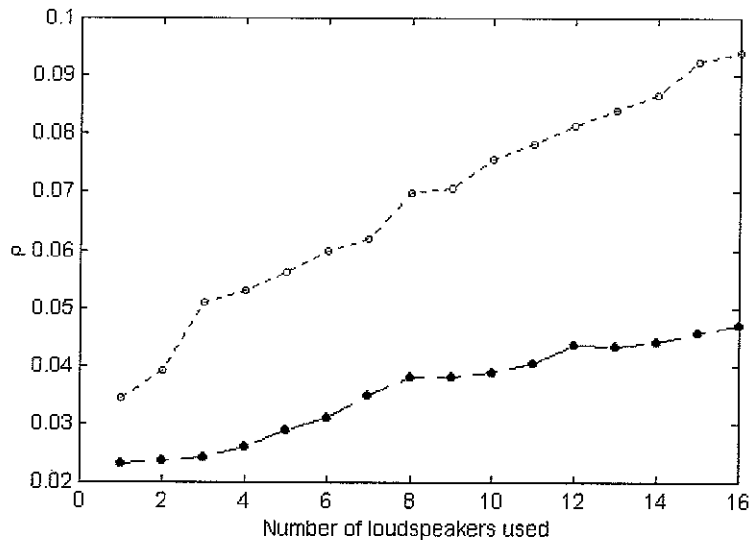


Figure 10. Size of the perturbation uncertainty as a function of the number of secondary sources used in the experimental enclosure. Optimal positions based on the perturbed plants: circle-dot line; optimal positions based on the nominal plant: point-dashed line

Comparing these values with those obtained in Figure 2, it is clear that both of them show the same trend, the perturbation size ρ , increases with the number of loudspeakers used in the system, but in this last case, these values are about half of the values obtained previously. Following the same procedure, once we have determine the nominal values and the perturbation size, the SDP software can be used to get the optimum robust effort control coefficient. This values, and the previous ones represented in Figure 3 are shown together in Figure 11.

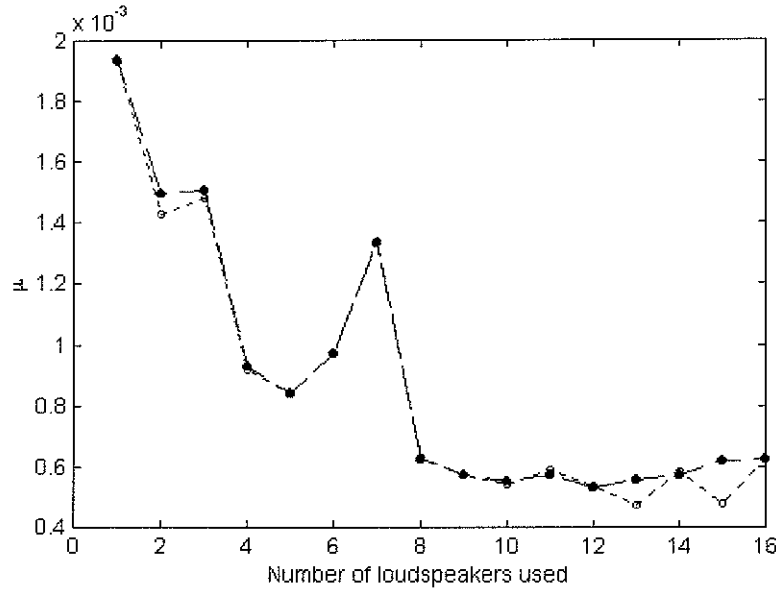


Figure 11. Optimal values of the effort coefficient, μ , vs. the number of secondary sources used. Optimal positions based on the perturbed plants: circle-dot line; optimal positions based on the nominal plant: point-dashed line

In an analogous manner to the previous section, the attenuation values obtained with the active control system are represented with and without including the leak parameter, first for the nominal plant, Figure 12, and then for the average perturbed plants, Figure 13.

From the comparison of these figures with Figures 7 and 8, respectively, it can be seen that the attenuation values obtained are very similar. The “nominal” values obtained in Figure 12, for the nominal plant, are clearly superior over the “robust” values, as in Figure 7. On the other hand, the trend observed in Figure 8 for the perturbed plants, it is not so clear in Figure 13. In this last case, although there are a few values that show better performance for the “robust” solution, in general, the “nominal” solution provides slightly higher levels of attenuation. So, the general conclusion of this section is that it looks more advantageous, from the robustness point of view, to use the measured plants in the physical system as much as possible for the determination of the nominal models.

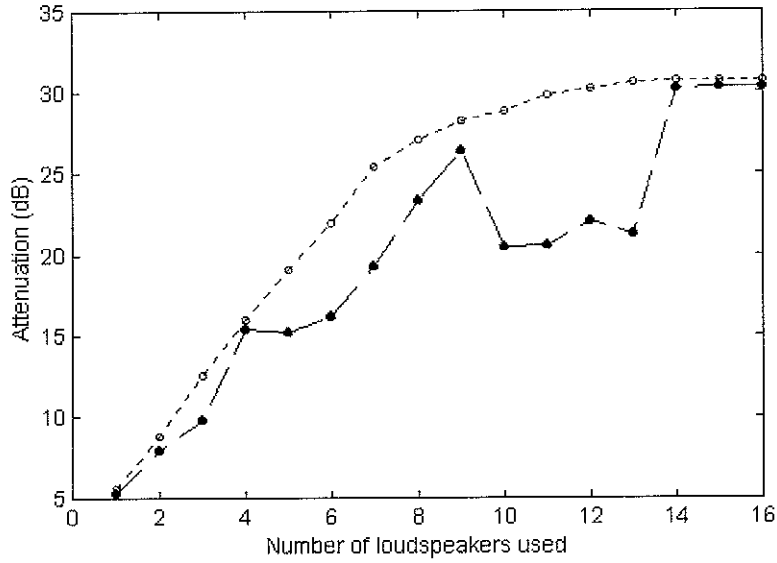


Figure 12. Attenuation values obtained as a function of the number of loudspeakers used in the active control system for the nominal plant. Effort parameter value μ equal to zero: circle-dot line; optimal values of μ in terms of performance: point-dashed line

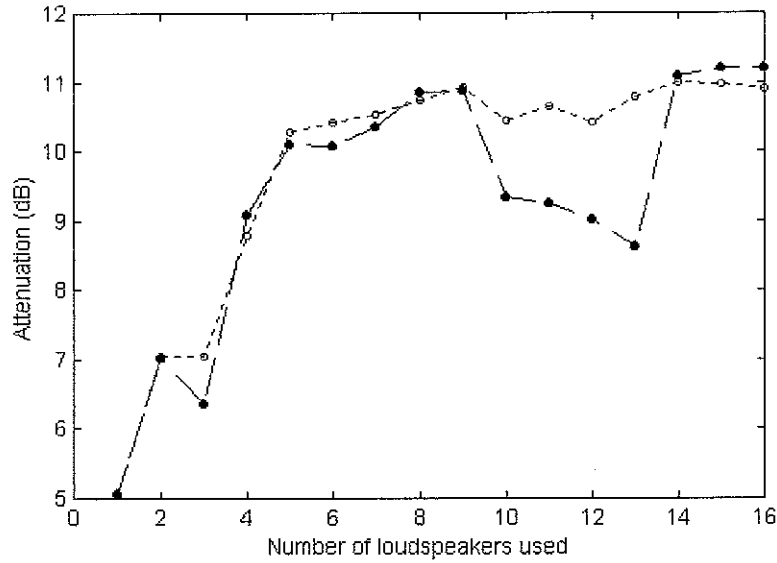


Figure 13. Attenuation values obtained as a function of the number of loudspeakers used in the active control system for the average perturbed plants. Effort parameter value μ equal to zero: circle-dot line; optimal values of μ in terms of performance: point-dashed line

5. Robust least squared solution of the problem

5.1 Theoretical formulation

As indicated in Section 3.2, in the mathematical formulation of the SDP problem it is assumed that the data \mathbf{G}_0 and \mathbf{d}_0 are given, and the optimum solution for the leak parameter, μ , is

obtained as a function of the perturbation size, ρ . Normally, in a real application we have a representation of the physical system that consists of a set of measured plants. In this case, the determination of the “nominal data” is not a straightforward process, and a lot of different criteria can be taken into account. Also, in some problems the norm bound ρ on the perturbation may be difficult to estimate. It would be very convenient to derive an alternative formulation to avoid the determination of all these parameters and to solve the problem just using the set of measured data obtained from the real system.

Another approach to the problem can be obtained trying to express the problem as the minimisation of a least-squares cost function. This is a very common and useful criterion that has been used, for example, in Section 2.2, to adjust the vector of secondary source strengths to minimise the sum of the error signal modules squared pressures. Following the formulation in this section, for each of the perturbed plants the complex vector of error signals is expressed as due to the primary source plus the contributions of the secondary sources as

$$\mathbf{e}_i = \mathbf{d}_i + \mathbf{G}_i \mathbf{u}_i \quad i = 1, \dots, 6 \quad (27)$$

A general formulation of the exact least-squares solution allows the complex vector of secondary source strengths to be expressed [10] as a matrix of the plant response multiplied by the primary field complex vector, as

$$\mathbf{u}_i = -\mathbf{G}_0^\dagger \mathbf{d}_i \quad (28)$$

where \mathbf{G}_0^\dagger is the pseudo-inverse of the matrix \mathbf{G}_0 , that depends on the particular problem considered. Substituting into equation (24), we obtain

$$\mathbf{e}_i = (\mathbf{I} - \mathbf{G}_i \mathbf{G}_0^\dagger) \mathbf{d}_i \quad (29)$$

If the cost function is defined as the sum of the complex vector of error signal, we have

$$J = \sum_{i=1}^6 \mathbf{e}_i^H \mathbf{e}_i = \sum_{i=1}^6 \mathbf{d}_i^H (\mathbf{I} - \mathbf{G}_0^{\dagger H} \mathbf{G}_i^H) (\mathbf{I} - \mathbf{G}_i \mathbf{G}_0^\dagger) \mathbf{d}_i \quad (30)$$

Using the properties of the trace of an outer product, this cost function can also be written

$$J = \text{trace}(J) \quad (31)$$

Expressing the equation in this way, we can try to use the results obtained for the differentiation of the trace of a matrix function with respect to the elements of one of the matrices in this function

$$J = \sum_{i=1}^6 \mathbf{d}_i^H \mathbf{d}_i - \text{trace} \sum_{i=1}^6 \mathbf{d}_i^H \mathbf{G}_0^{\dagger H} \mathbf{G}_i^H \mathbf{d}_i - \text{trace} \sum_{i=1}^6 \mathbf{d}_i^H \mathbf{G}_i \mathbf{G}_0^{\dagger} \mathbf{d}_i + \text{trace} \sum_{i=1}^6 \mathbf{d}_i^H \mathbf{G}_0^{\dagger H} \mathbf{G}_i^H \mathbf{G}_i \mathbf{G}_0^{\dagger} \mathbf{d}_i \quad (32)$$

Unfortunately, using the properties of the trace of a matrix we are not able to simplify the last term of equation (27) so that it becomes easily differentiable. But it is still possible to obtain an analytical solution to the problem if, instead of minimise the sum of the complex vector of error signals, $\sum_{i=1}^6 \mathbf{e}_i^H \mathbf{e}_i$, we minimise the sum of the complex vector of error signals, normalised by

the primary field, $\sum_{i=1}^6 (\mathbf{e}_i ./ \mathbf{d}_i)^H (\mathbf{e}_i ./ \mathbf{d}_i)$, where the symbol “./” denotes an element by element division. Equation (27) and (29), then, are transformed, respectively

$$J = \sum_{i=1}^6 (\mathbf{e}_i ./ \mathbf{d}_i)^H (\mathbf{e}_i ./ \mathbf{d}_i) = \sum_{i=1}^6 (\mathbf{I} - \mathbf{G}_0^{\dagger H} \mathbf{G}_i^H)(\mathbf{I} - \mathbf{G}_i \mathbf{G}_0^{\dagger}) \quad (33)$$

$$J = \sum_{i=1}^6 \mathbf{I} - \text{trace} \sum_{i=1}^6 \mathbf{G}_0^{\dagger H} \mathbf{G}_i^H - \text{trace} \sum_{i=1}^6 \mathbf{G}_i \mathbf{G}_0^{\dagger} + \text{trace} \sum_{i=1}^6 \mathbf{G}_0^{\dagger H} \mathbf{G}_i^H \mathbf{G}_i \mathbf{G}_0^{\dagger} \quad (34)$$

Introducing this modification, and using the properties of the trace of a matrix, the derivative of the cost function J with respect to the real and imaginary parts of \mathbf{G}_0^+ can be expressed as

$$\frac{\partial J}{\partial \mathbf{G}_{0R}^{\dagger}} + j \frac{\partial J}{\partial \mathbf{G}_{0I}^{\dagger}} = 2\mathbf{G}_0^{\dagger H} \sum_{i=1}^6 \mathbf{G}_i^H \mathbf{G}_i - 2 \sum_{i=1}^6 \mathbf{G}_i \quad (35)$$

Once we have expressed the error criteria as a quadratic function of the variable of interest and we have differentiated with respect to that variable, it is necessary to set the gradient of the derivative to zero to find the optimum value of the variable, which results

$$\mathbf{G}_0^{\dagger H} = \left(\sum_{i=1}^6 \mathbf{G}_i \right) \left(\sum_{i=1}^6 \mathbf{G}_i^H \mathbf{G}_i \right)^{-1} \quad (36)$$

Once we have obtained the solution for the pseudo-inverse matrix, we can go back to the original equation (24), for the complex vector of error signals, and calculate the attenuation values provided by the particular configurations. When the number of measured perturbed transfer function is only one, the optimal robust pseudo-inverse matrix is the same as the solution obtained in Section 2.2, as it would be expected.

5.2 Numerical simulations

A set of simulations has been carried out to validate and check the accuracy of the robust least squares solution. In order to compare the attenuation results provided by the solution of the SDP problem, when the leak parameter is adjusted to optimise the robust performance, and the solution provided in the previous section, the attenuation results have been plotted against the number of loudspeakers used in the control systems, together with the results obtained previously.

The comparison has been made with the results obtained in Section 4.3, when the average perturbed plants were used by the simulated annealing algorithm to optimise the positions of the transducer in the control system, because they provide slightly better results in terms of robustness performance. Using equation (23), the attenuation values for the average perturbed plants obtained with the robust least squares solution and the SDP solution have been represented in Figure 14.

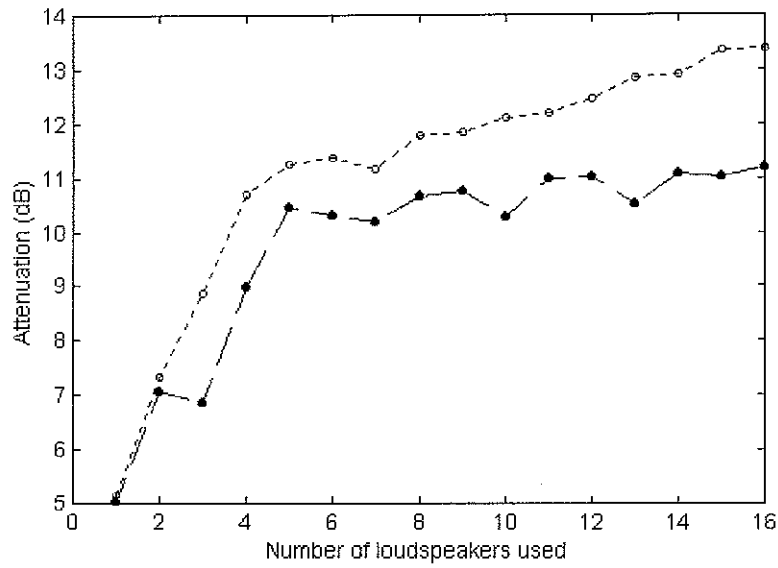


Figure 14. Attenuation values obtained as a function of the number of loudspeakers used in the active control system from the average of the perturbed plants. Robust least-squares solution: circle-dot line; SDP solution: point-dashed line

Both representations are similar and show the same trends, but the attenuation values provided by the robust least squares solution are higher than those provide by the solution of the SDP algorithms, as this last results is more general, and is not specific to any type of perturbed plants. On the other hand, when the robust least squares solution is used with the nominal plant, the situation is reversed, as shown in Figure 15.

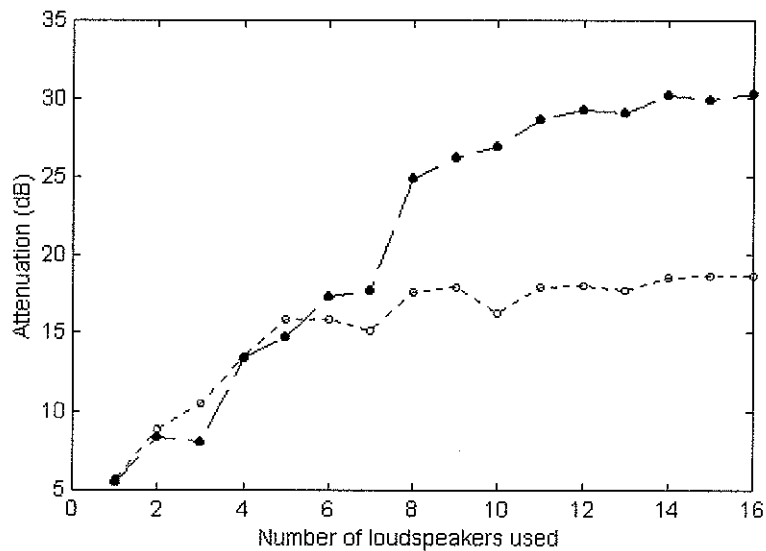


Figure 15. Attenuation values obtained as a function of the number of loudspeakers used in the active control system for the nominal plant. Robust least-squares solution: circle-dot line; SDP solution: point-dashed line

From these two figures, it seems that the robust least squares solution is able to provide good results only when used in the set of perturbed plants used to derive the robust pseudo-inverse matrix, whereas it does not work so well when with other plants not include in the solution. The mathematical solution obtained with the SDP problem seems to perform well in all type of situations, although the determination of the nominal values could be a difficult and time-consuming process.

6. Summary and conclusions

The main concern of this work has been to study the effects of the presence of uncertainty and the performance of an active noise control system, and to find methods to alleviate this problem through the formulation of robust performance controllers. Some work has been carried out previously to study the optimal transducer positions in a rectangular enclosure using the simulated annealing algorithm. In this occasion, the attention was focussed in the selection of the positions that were more resistant to plant variations, caused, for example, by the presence or absence of objects inside the enclosure. Some modifications were included in cost function used by the algorithm to select the configurations that provided good attenuation levels with low control effort values. The weighting factor used was chosen as a trade-off between these two factors, for the particular configurations selected. The results obtained were only slightly smaller than in the case of using the nominal plant.

The purpose of this work is to continue in this subject of research, using now a mathematical formulation for robust solutions to least-squares problems with uncertainty data. Following the approach of Fonseca et al. [4] for the formulation of the stability and performance of the LMS algorithm, it is possible to select the optimal choice of the weighting effort control parameter in terms of robustness.

Using a set of measured perturbed plants in a laboratory enclosure, a computational algorithm has been presented to select the nominal plant and the size of the perturbation in the control system. The optimal leak parameter as a function of the number of loudspeakers used has been calculated using a software package for solving standard SDP problems, and performance results have been obtained for the nominal plant and for the average perturbed plants. In the first case, the nominal solution (leak parameter μ equal to zero) provides better attenuation than when effort control is introduced in the system, and the situation is reversed for the average perturbed plants. It is important to note that in this case, the values of the attenuation obtained when the average perturbed plants are used are less than half the values obtained with the

nominal plant. It has been also shown that, from the robustness point of view, it is more convenient to work as much as possible with the perturbed plant for the determination of the nominal data.

Finally, a robust least square solution for the problem is presented, and an analytical solution is deduced when the sum of the complex vector of error signals normalised by the primary field is minimised. The performance results obtained in this case show good agreement for the average perturbed plants, but not with the nominal plant.

The control signals are assumed to be calculated off-line in this report, but in practice would be adapted using an on-line iterative algorithm. An additional constraint, not considered here, would be the need for stability in this algorithm

7. References

1. Elliott, S. J., Stothers, I. M and Nelson, P. A., 1987. *A multiple error LMS algorithm and its application to the active control of sound and vibration*. IEEE Trans. Acoust., Speech and Signal Processing, ASSP-35, 1423-1434
2. Boucher, C. C., Elliott, S. J. and Nelson, P. A., 1991. *The effects of modelling errors on the performance and stability of active noise control systems*. Proceedings in the Recent Advances in Active Control of Sound and Vibration, Blacksburg, VA, 290-301
3. Omoto, A. and Elliott, S. J., 1999. *The effect of structured uncertainty in the acoustic plant on multichannel feedforward control systems*. IEEE Trans, Signal Processing, 7 (2), 204-212
4. Fonseca, P., Sas, P. and Brussel, H. V., 2001. *Robust design and robust stability analysis of active noise control systems*. Journal of Sound and Vibration, **243** (1), 23-42
5. El Ghaoui, L. and Lebret, H., 1997. *Robust solution to least-squares problems with uncertain data*. SIAM Journal of Matrix Analysis and Applications, **18**, 1035-1064
6. Bravo, T. and Elliott, S. J., 1999. *The selection of robust and efficient transducer locations for active sound control*. ISVR Technical Memorandum No. 843
7. Nelson, P. A. and Elliott, S. J., 1992 **Active Control of Sound**. London: Academic Press
8. Baek, K. H., 1996. *Non-linear optimisation problems in active control*. Thesis doctoral. ISVR, University of Southampton.
9. Kirkpatrick, S., Gelatt, C. D. and Vecchi, M. P. 1983. *Optimisation by simulated annealing*. Science **220**, 671-680.

10. Toh, K. C., Todd, M. J. and Tutuncu, R. H., 1999. *SDPT3: A Matlab software package for semidefinite programming*. Available from <http://www.math.cmu.edu>
11. Elliott, S. J., 2001. **Signal processing for active control**. Academic Press, London